ELSEVIER

Journal of Power Sources 81–82 (1999) 54–59

JOURNAL OF POWER SOURCES

www.elsevier.com/locate/jpowsour

An update on the high temperature ageing mechanism in $LiMn_2O_4$-based Li-ion cells

A. du Pasquier [a,b,*], A. Blyr [a,b], A. Cressent [a,b], C. Lenain [a,b], G. Amatucci [a,b], J.M. Tarascon [a,b]

[a] *Laboratoire de Reactivite et de Chimie des Solides, UPRES-A 6007, France*
[b] *UPJV, 33 rue Saint Leu, 80039, Amiens, France*

Abstract

$LiMn_2O_4$-based Li-ion cells suffer from a limited cycle-life and a poor storage performance at 55°C, both in their charged and discharged states. From 3-electrode type electrochemical measurements, the non-stability of $LiMn_2O_4$ in electrolytes containing traces of HF was identified as being the source of such a poor performance. To get some insight in the mechanism by which the high-temperature ageing proceeds, a survey of the chemical stability of high surface area $LiMn_2O_4$ in various Li-based electrolytes was performed as a function of temperature. The growth of a protonated λ-MnO_2 phase was identified when $LiMn_2O_4$ powders were stored into the electrolyte at 100°C for several hours. Such a protonated phase is partially inactive with respect to lithium intercalation, thereby accounting for some of the irreversible capacity loss experienced at 55°C for $LiMn_2O_4$-based Li-ion cells.

Keywords: Lithium; Batteries

1. Introduction

The production of rechargeable Li-ion $LiCoO_2$/C cells [1] is rapidly increasing to meet the hungry portable market demand. Such commercial success has prompted research towards better electrode materials for both positive and negative electrodes, and new materials were found. Vanadates and recently Sn-based oxides have been proposed as an alternative to the presently used graphite negative electrodes [2]. With respect to the positive materials, the mixed $LiNi_{1-x}Co_xO_2$ phase [3] presently stands as a serious contender to replace $LiCoO_2$, while intense effort is still devoted towards improving the limited high temperature performance of the $LiMn_2O_4$/C Li-ion system in its charged state. Improvements have been made [4–6], however, they are not sufficient to ensure its wide acceptance by battery manufacturers. More importantly, during this study we did unravel that the high temperature ageing issue was not only limited to the charged state of the $LiMn_2O_4$/C Li-ion cell [7,9], but was persisting (Fig. 1) whatever the state of charge of the battery (e.g., fully discharged or fully charged).

We have recently been addressing this issue [8] by means of electrochemical measurements coupled with chemical simulations in order to (1) determine the mechanism by which this detrimental ageing reaction is occurring, and (2) hopefully provide a solution to this recurrent problem. By means of various electrochemical tests we already showed that the limited high-temperature performance was mainly associated to the $LiMn_2O_4$ electrode and more specifically to its instability towards Mn dissolution. To further throw some light on the origin of this observed instability we embarked in a complete chemical study consisting in determining the key experimental parameters governing Mn dissolution. Here, we mainly reported on such a chemical simulation approach with special attention on the effect of the spinel surface area as well as the amount and nature of the electrolyte on the Mn dissolution. We unravelled the formation of a protonated phase that grows with increasing the storage time at high temperature, and gives evidence for a qualitative correla-

* Corresponding author

0378-7753/99/$ - see front matter
PII: S0378-7753(99)00136-6

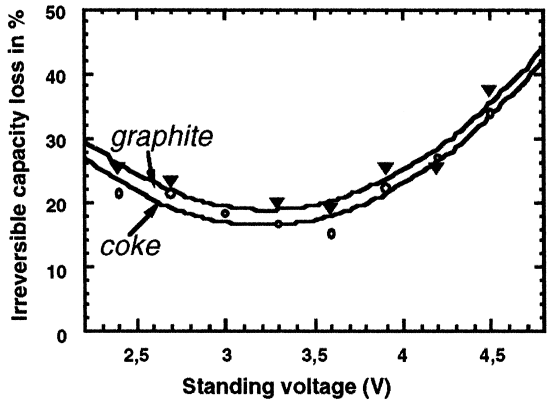

Fig. 1. Variation of the irreversible capacity cumulated over four subsequent weeks at 55°C for $LiMn_2O_4$/C (C = coke or graphite) Li-ion cells stored at various voltages (e.g., state of charge).

tion between the amount of capacity loss and the amount of protonated phase.

2. Experimental

$Li_{1.05}Mn_{1.95}O_4$ powders with surface areas of either 0.8 m^2/g or 5 m^2/g were prepared by reacting stoichiometric amounts of EMD-MnO_2 at 800°C with Li_2CO_3 and $LiNO_3$, respectively, as previously reported (4). The Li rich spinels $Li_{1+x}Mn_{2-x}O_4$ $(0.1 < x < 0.35)$ were made by reacting stoichiometric amounts of $LiNO_3$ and λ-MnO_2 at temperatures ranging from 400°C to 750°C depending on the values of x as reported in Ref. [10]. Delithiation of the above phases was made according to the acid leaching technique recognized by Hunter [11].

Chemical simulation studies of 0.8 m^2/g $LiMn_2O_4$ powders towards Mn dissolution were mainly done at various temperatures by mixing 0.5 g of $LiMn_2O_4$ powders with 10 cm^3 of the selected electrolyte (mainly 1 M $LiPF_6$ in 1-1 EC-DMC by volume), and by placing the solutions in hermetically sealed metallic plastic bags or in teflon containers within a hermetically sealed plastic bag for various periods of time.

The resulting recovered $LiMn_2O_4$ aged powders, after separation from the electrolyte by centrifugation and several DMC washes, were characterized by various techniques such as X-ray diffraction using a Philips diffractometer ($Cu_{k\alpha 1}$ radiation), and scanning electron microscopy (SEM) using a Philips FEG-XL30 having an EDX facility. Chemical analyses on the aged $LiMn_2O_4$ powders or on the supernatant electrolytes were done by Atomic Absorption Spectroscopy (AAS) using a 3030 Perkin-Elmer. Mn oxidation degree on the solid was determined by chemical titration, and the electrolyte HF content by an acid-base titration. BET surface area with N_2 adsorption was obtained from a Micrometrics Gemini 2370. Infrared spectra in KBr pellets were collected from a Nicolet 510 Fourier transform infrared spectrophotometer. Thermal gravimetric analysis measurements were carried out using a Mettler (TC11) equipment.

The electrochemical measurements vs. Li were done using Swagelok™ cell hardware. The positive composite electrode was made within the dry box by intimately mixing $LiMn_2O_4$ with SP powders, and directly placing them into the aluminium Swagelok™ plunger, followed by cell assembly. For protons intercalation a three-electrode cell using Hg/HgO as the reference, platinum as the counter electrode, MnO_2 material mixed with carbon as the working electrode, and 6 M KOH as electrolyte was used. Both Swagelok™ and 3-electrode cells were cycled by means of a Mac-Pile system (Bio-Logic, Claix, France) operating in a galvanostatic mode.

3. Results

We first pursued a study of several parameters on the amount of Mn and HF into the electrolyte as a function of the storing time of a 0.8 m^2/g powder into a 1 M $LiPF_6$ (1:1, EC-DMC) electrolyte, and measured a simultaneous increase in the amount of HF and dissolved Mn present in the electrolyte when (1) using $LiPF_6$ instead of $LiBF_4$, $LiClO_4$, and $LiAsF_6$, (2) increasing both the salt concentration and the volume of electroyte used, and (3) increasing the storage temperature.

Electrochemical measurements performed on these samples have revealed a decrease in the cell capacity together with an increase in polarisation at a given temperature with increasing the storage time or, for the same storage time with increasing the temperature. These observations suggested the formation of a passivating film on $LiMn_2O_4$ particles that was separately confirmed by scanning electron microscopy.

Finally, a series of samples stored in the electrolyte at 100°C for various amounts of time did indicate the presence of a shoulder on the side of each main Bragg peak, which intensity was increasing with increasing temperature. Attempts to increase the contribution of this phase by leaving the samples for longer time at 100°C did not succeed, suggesting a diffusional limited process. Based on our previously reported finding that Mn dissolution is enhanced with increasing the spinel surface area, we decided in order to favor the formation of this new phase that is the result of the Mn dissolution, to conduct a similar series of experiments using a spinel of 5 m^2/g instead of 0.8 m^2/g.

As before, the 5 m^2/g $LiMn_2O_4$ powders were stored at 100°C into a 1 M$LIPF_6$ (1:1, EC-DMC) electrolyte for various periods of time, and the resulting products (each separated into two equal batches denoted A and B) were characterized for their structural and electrochemical properties. The evolution of the X-ray powder patterns for these samples is shown on Fig. 2. Note a continuous shift

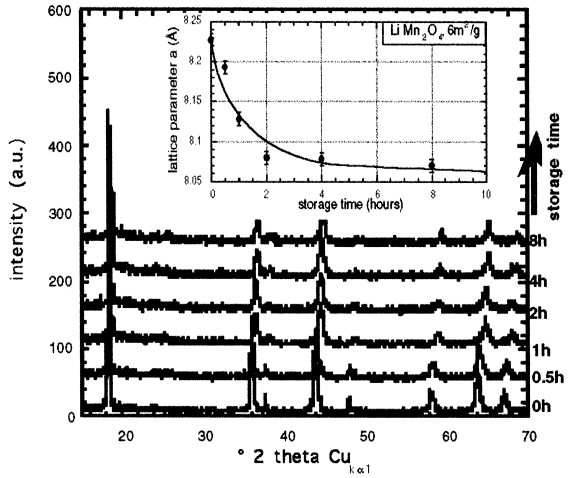

Fig. 2. Evolution of the X-ray powder diffraction patterns for $LiMn_2O_4$ samples stored in electrolyte at 100°C for various amounts of time.

of the Bragg peaks with increasing storage time implying a monophasic process. The cubic *a*-axis continuously decreases to reach a value similar to that of λ-MnO_2, the reason why we will refer to this phase as a 'λ-MnO_2-type phase'. An IR study of these powders indicated organic bands suggesting the organic nature of the passivating layer forming around each particle, however, difficulties were encountered in determining its exact composition. This passivating layer can be dissolved in water and AAS analyses of the resulting water solution revealed large amounts of both Mn and Li. Usually, the amount of Mn content measured in the passivating layer was greater than in the electrolyte. Finally, we experienced that the Mn partition between the passivating layer and the electrolyte strongly depends upon the nature of the electrolyte (Fig. 3). For instance when 1 M $LiBF_4$ in 1:1 EC-DMC was used as a storage electrolyte, the amount of Mn measured in the passivating layer had an order of magnitude greater than the one measured in the electrolyte.

The washed samples were further investigated by IR measurements, and the disappearance of the organic coating was confirmed but, more importantly, an extra line located at 908 cm^{-1} and growing with increasing storage time at 100°C was observed. A similar band was recently reported by Ammundsen et al. [12,13] for protonated delithiated Li-rich spinel samples ($H_zLi_xMn_{2-y}O_4$), and was ascribed to hydroxyl groups (e.g., the presence of protons) within the framework structure. For comparison purposes Li-rich spinel samples $Li_{1+x}Mn_{2-x}O_4$ ($0 < x < 0.35$) were made, delithiated in acidic media (to produce the series of samples denoted C), and investigated by IR spectroscopy. Fig. 4 shows a close similarity between the IR spectra of the electrolyte aged sample and the delithiated Li-rich spinel phase, strongly suggesting that the new phase forming upon storage is a protonated Mn-deficient spinel phase of general formula (λ-$H_zMn_{2-x}O_4$). The presence of protons was further confirmed by conducting TGA measurement. For the unwashed samples, the TGA derivative curve exhibits two peaks at about 140°C and 500°C, that were ascribed to the release of CO_2 and O_2 ($Mn_2O_4 \rightarrow Mn_2O_3 + 1/2O_2$), respectively, with occasionally one at 550°C which origin is not yet completely determined. The TGA derivative curve for the washed samples is quite similar with the only difference that the peak at 140°C corresponding to the burning of the organics is gone to the expense of another peak that was previously masked, and corresponding to the departure of water at a slightly greater temperature (Fig. 5). The similarity between the TGA

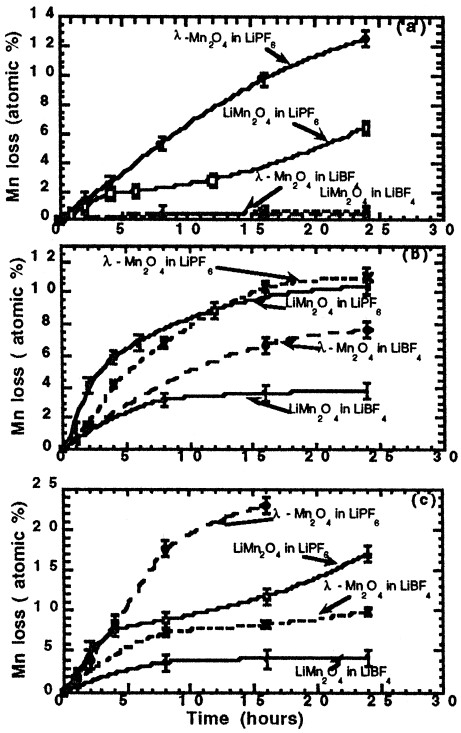

Fig. 3. Mn Content measured in the electrolyte (a), in the passivating layer (b), and Mn total loss upon storage (c).

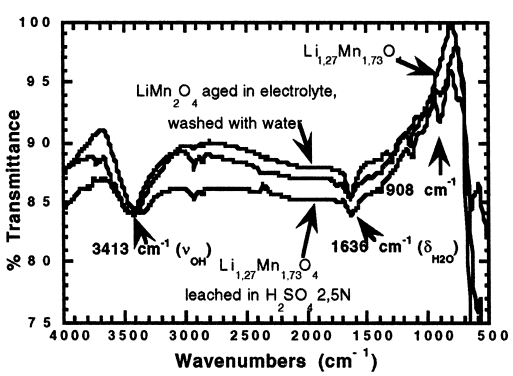

Fig. 4. IR spectra for as made $Li_{1.27}Mn_{1.73}O_4$, acid leached $Li_{1.27}Mn_{1.73}O_4$ and $LiMn_2O_4$ stored at 100°C into the electrolyte for 12 h.

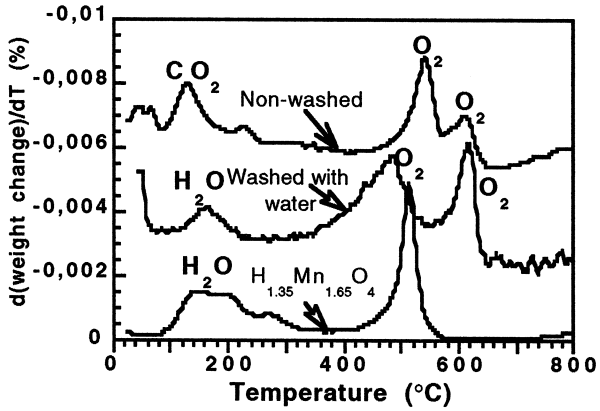

Fig. 5. The TGA derivatives for a water washed and unwashed $LiMn_2O_4$ sample stored for 24 h at 100°C in the electrolyte are compared with that of a C sample.

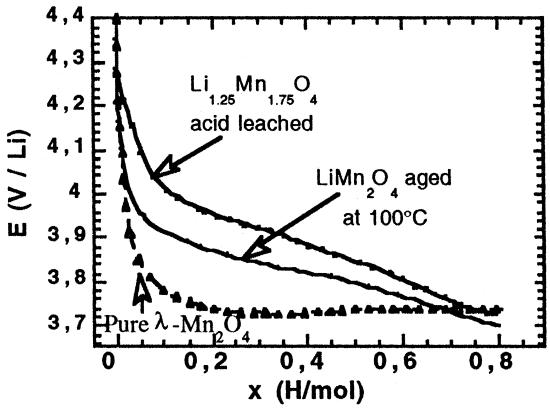

Fig. 7. Voltage vs. composition curve for a proton cell using λ-MnO_2, acid leached $Li_{1.25}Mn_{1.75}O_4$ and a $LiMn_2O_4$ stored sample. (The potentials are given vs. Li).

derivatives collected for the C series and for our high temperatures aged samples confirm our proton argument.

All these samples were electrochemically characterized. The unwashed samples show a greater polarization and a smaller capacity than the washed samples (Fig. 6). This is as expected due to (1) the diffusion limiting passivating layer that enhances the polarization and (2) the dead weight of this layer with respect to the intercalation that results in a lowering of the reversible capacity. We note, however, that even after the washing step our samples do not fully recover their initial capacity. We did perform electrochemical measurements vs. Li for the C series, and indeed showed that the samples having the largest amount of protons (e.g., of Mn vacancies) are those that reversibly insert the less amount of lithium in agreement with Ammundsen's work. This observation further supports the formation of a protonated phase upon high temperature storage of $LiMn_2O_4$ powders.

As an ultimate attempt to prove that our aged material was a protonated deficient λ-MnO_2 phase we did investigate the intercalation of protons for pure λ-MnO_2 sample, for samples of the C series and for our high temperature electrolyte aged materials (Fig. 7). The shape of the voltage composition curve for our high temperature electrolyte aged sample, showing a continuous slight dropping of the voltage upon proton uptake, turns to be closer to that of a C series sample than that of a pure λ-MnO_2 sample.

Knowing (1) the amount of Li and Mn in the resulting washed material (as determined by AAS and confirmed by electrochemical analysis) and (2) the oxidation degree of Mn we could attempt to roughly estimate the proton

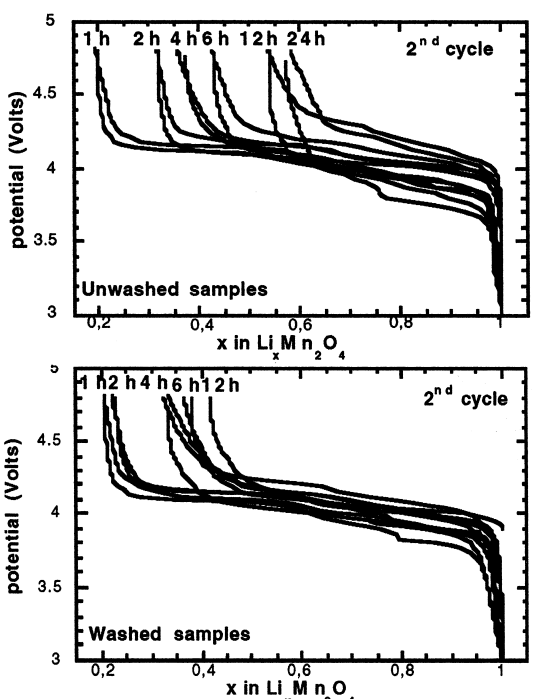

Fig. 6. Voltage vs. composition curve vs. Li for unwashed and washed $LiMn_2O_4$ samples stored in the electrolyte at 100°C for various lengths of time.

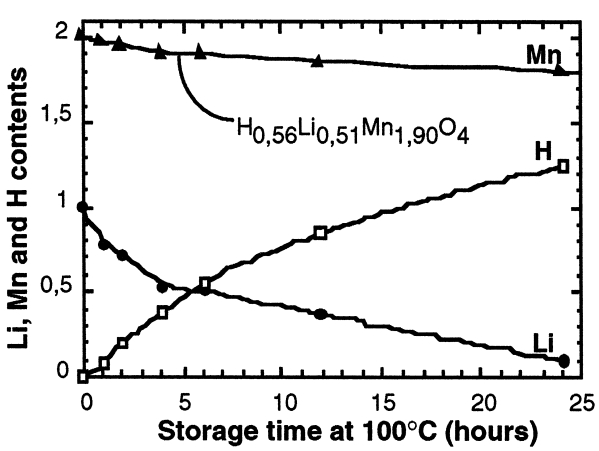

Fig. 8. Mn, Li, and protons content for $LiMn_2O_4$ powders stored at 100°C for various amounts of time.

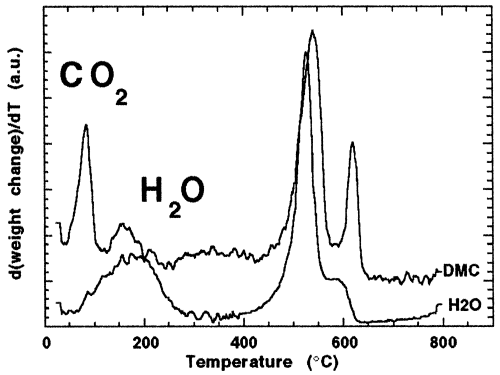

Fig. 9. The TGA derivatives are shown for a washed and unwashed λ-MnO_2 sample aged at 100°C into the electrolyte.

content for our 100°C $LiMn_2O_4$ aged samples as function of time (Figs. 8 and 9). The amount of protons estimated from these calculations reasonably agree with the proton content deduced by TGA measurement.

At this point, a legitimate question is whether the formation of a protonated phase does also occur when λ-MnO_2 instead of $LiMn_2O_4$ is stored at high temperature into 1 M $LiPF_6$ (1:1,EC-DMC) electrolyte. A study similar to the one described above was duplicated using chemically made λ-MnO_2 samples (5.0 m^2/g). The general trends previously established remain. The main difference only resides in the observation that the Mn dissolution is always larger for λ-MnO_2 than for $LiMn_2O_4$.

Interestingly, the TGA derivative collected on non water washed λ-MnO_2 phase samples distinctly revealed the CO_2 and H_2O peaks, rejecting the possible argument that protonation did only occur during the water washing treatment.

Finally, a remaining conflicting result was the detection of only tiny amounts of Mn when $LiMn_2O_4$ powders were left into electrolytes using $LiAsF_6$, $LiBF_4$ or $LiCLO_4$ salts instead of $LiPF_6$, while three-electrode Li-ion cells using such an electrolyte revealed limited high temperature performances. To clarify this point, studies were done on $LiMn_2O_4$ and on λ-MnO_2 powders as before, but using $LiBF_4$ instead of $LiPF_6$ and while keeping the same electrolyte solvent (EC-DMC in the 1:1 ratio). When $LiMn_2O_4$ was left under storage at 100°C, the Mn dissolution was found to be three to four times less with, in addition, quite a different partition since most of the Mn was found to reside in the passivating layer, consistent with the small numbers previously announced into the electrolyte. Overall the Mn loss is smaller, the reason why the capacity loss upon storage is smaller than for $LiPF_6$ samples stored for the same amount of time. In contrast, with λ-MnO_2, we did observe a larger increase in the Mn dissolution comparable to what was measured when using $LiPF_6$. This effect is most likely due to the poor stability of $LiBF_4$-based electrolyte with respect to $LiPF_6$ electrolyte against oxidation at high voltages.

4. Discussion

We reported on the influence of various parameters on the instability of both $LiMn_2O_4$ or delithiated spinel towards Mn dissolution into an electrolyte at 100°C. Among the main results are that (1) Mn dissolution increases with increasing temperature, volume and electrolyte concentration, and is enhanced for the delithiated samples compared to the lithiated ones consistent with the observation that the capacity loss was slightly larger when the cell was left on storage in its charged state (λ-MnO_2) rather than in its discharged state ($LiMn_2O_4$), and (2) this Mn dissolution is not specific to $LiPF_6$, but does exist with other salts with however some variations. For instance with $LiBF_4$, such dissolution was found to be quite more severe for the delithiated than for the lithiated phase.

All the presented data, namely the one showing that Mn dissolution and HF content increase simultaneously, imply the importance of acids in promoting this reaction. Such acids can be generated from either salt or solvent decomposition. $LiPF_6$ for instance is known [14,15] to be thermally unstable, and to decompose into LiF and PF_5 species that can be hydrolyzed with traces of water to give HF ($PF_5 + H_2O \rightarrow 2HF + POF_3$; (reaction 1)). The amount of HF, thus generated from the salt decomposition, is expected to strongly change with the nature of the salt consistent with our experiments that indicate a less severe Mn dissolution for $LiBF_4$ that is more thermally stable than $LiPF_6$. Organic solvents such as ethers or carbonates [16] can also be oxidized by λ-MnO_2, either directly ($R-H \rightarrow R^\circ + e^- + H^+$ (reaction 2)) or via radical intermediates generated from the Li-salt anion. The main result of these processes is the formation of a passivating organic/inorganic coating of the spinels particles and the generation of protons in the medium. In the light of the above reactions, one can anticipate depending upon which of the processes (1) or (2) is predominant, that Mn dissolution can be greater in the charged than in the discharged state or vice versa. With $LiPF_6$ reaction (1) is expected to be the most predominant thus one can expect a high Mn dissolution in the discharged state (e.g., when $LiMn_2O_4$ is placed into the electrolyte). In contrast, for $LiBF_4$, due to both the documented enhanced thermal stability of the salt and its lower stability against oxidation at high voltages, reaction (2) should be favored with respect to reaction (1). On this basis, the larger Mn dissolution observed for λ-MnO_2 rather than for $LiMn_2O_4$ when both are placed at 100°C in 1 M $LiBF_4$-EC-DMC electrolyte can be explained. Finally, we have shown that for our high temperature aged samples, Mn dissolution was concomitant with the uptake of protons resulting in the formation of a λ-protonated phase that is partially electrochemically inactive, consistent with Ammundsen's results, thereby enabling to account for irreversible capacity losses observed.

For this protonation to occur, based on Ammundsen's work, one must pass during the ageing process by a Li rich

spinel (e.g., a Mn deficient spinel). Such a requirement simply eliminates Hunter's reaction since this reaction, while leading to Mn dissolution, results in a stoichiometric spinel with no vacancies on the 16d sites. Thus, a possible scenario to account for the ageing mechanism can be as follows: first, in acidic media, we have the formation of a deficient spinel phase $Li_{1+2y}Mn_{2-y}O_4$ mediated from the ion exchange of Mn^{+2} for 2 Li^+ or for protons and lithium simultaneously. Then, once all the Mn reach the $+4$ oxidation state, an ion exchange of H^+ for Li^+ takes place so that we end up with a protonated phase that partially electrochemically intercalates lithium thus leading to a capacity loss and an increase in polarisation. Such a scenario is very attractive since it will simultaneously account for the Mn dissolution, the obtention of a deficient Mn spinel, and the uptake of a proton as well as for the formation of a passivating layer composed of Mn and Li (Li moving towards the particle surface when protons move towards the core of the material during exchange). However, some ambiguity still remains with respect to the way that the initial ion exchange reaction leading to the Mn deficient spinel proceeds, since we called upon a quite unusual reaction in solid state chemistry that is the ion exchange of 2 monovalent cations for one divalent cation.

5. Conclusion

A survey of various parameters influencing the stability of both $LiMn_2O_4$ and λ-MnO_2 towards Mn dissolution enables us to propose a mechanism that links the capacity losses encountered within the $LiMn_2O_4$/Li ion cells at high temperatures to the presence of acids/proton within the electrolyte that enables the formation of a Mn deficient spinel, and thereby its protonation to produce a partially inactive protonated Mn-deficient spinel phase. Neutron work presently in progress on samples aged in deuteriated electrolytes should enable to localize the protons sites within the spinel framework, and throw some light on their behavior with respect to Li reintercalation. Being able to partially explain the mechanism by which the Li-ion cells rapidly fades at high temperatures, we open new avenues of research to improve the performance of such a system. Besides the ones previously tried dwelling with decreasing the Mn dissolution by surface treatments/coatings, or by increasing the stability of the spinel towards Mn dissolution, we have investigated the use of chemical additives, such as zeolites that could trap protons or water molecules as they formed. This approach turned-out to be very successful as will be reported elsewhere. Besides its practical importance this result re-inforces our proposed mechanism that associated capacity losses to Mn dissolution are concomitant with the formation of a protonated phase.

References

[1] T. Nagaura, K. Tazawa, Prog. Batteries Sol. Cells 9 (1990) 20.
[2] Y. Idota, ERur. Pat. 0-567-149 A1, 1993.
[3] T. Ohzuku, A. Ueda, M. Nagayama, Y. Iwakoshi, H. Komori, Electrochim. Acta 38 (1993) 1159–1167.
[4] J.M. Tarascon, US Patent, 6, 295-714.
[5] Y. Xia, Y. Zhou, M. Yoshio, J. Electrochem. Soc. 144 (1997) 2593–2600.
[6] G.G. Amatucci, A. Blyr, C. Sigala, P. Alfonse, J.-M. Tarascon, Solid State Ionics 104 (1997) 13–25.
[7] A. Blyr, C. Sigala, G.G. Amatucci, D. Guyomard, Y. Chabre, J.-M. Tarascon, J. Electrochem. Soc. 145 (1998) 194.
[8] A. Blyr, A. Du Pasquier, G. Amatucci, J.-M. Tarascon, Ionics 3 (1997) 321.
[9] A. DuPasquier, A. Blyr, P. Courjal, D. Larcher, G. Amatucci, B. Gérand, J.M. Tarascon, J. Electrochem. Soc., in press.
[10] P. Endres, A. Ott, S. Kemmler-Sack, H.A. Mayer, H.-W. Praas, K. Brandt, J. Power Sources 69 (1997) 145–156, [17].
[11] J.C. Hunter, J. Solid State Chem. 39 (1981) 142.
[12] B. Ammundsen, D.J. Jones, J. Rozière, Chem. Mater. 7 (1995) 2151–2160.
[13] B. Ammundsen, P.B. Aitchinson, G.R. Buruns, D.J. Jones, J. Rozière, Solid State Ionics 97 (1997) 269–276.
[14] D.H. Jang, S.M. Oh, J. Electrochem. Soc. 144 (1997) 3342–3348.
[15] D. Aubarch, A. Zaban, A. Schlecter, Y. Ein-Eli, E. Zinigrad, B. Markowsky, J. Electrochem. Soc. 142 (1995) 2873.
[16] K. Kanamura, S. Toriyama, S. Shiraishi, Z. Takehara, J. Electrochem. Soc. 144 (1997) .